Optimal design of 2-D and 3-D shaping for linear ITG stability*

Mordechai N. Rorvig[1†],
in collaboration with
Chris C. Hegna[1], Harry E. Mynick[2], Pavlos Xanthopoulos[3], and M. J. Pueschel[1]

[1]University of Wisconsin, Madison, WI, USA
[2]Princeton Plasma Physics Laboratory, Princeton, NJ, USA
[3]Max-Planck-Institut für Plasmaphysik, Greifswald, Germany

Columbia University
13 September, 2013, New York, NY

† contact : rorvig@wisc.edu
***Supported by U.S. DoE grants DE-FG02-99ER54546 and DE-SC0006103.**

Overview of results

i. Design targets

- The targets provide an analytic, quantitative metric for the relation between the geometry and the ITG instability.

ii. Optimal design mechanisms

- The essential mechanisms by which the shaping controls the targets are investigated.

iii. Example calculations

- Example calculations build a framework for understanding.
- Show we can analytically predict & explain trends in the maximum linear growths rate from GENE.

Thus, a clear path to ITG optimization is shown.

A simpler approach to understanding 3-D shaping effects is needed

- **Success in neoclassical optimization has given rise to interest in turbulence optimization using shaping**
  - Linear growth rate provides a natural "cost function"
    - However, seemingly vast parameter space
    - What and how we should optimize is unclear.
- **Thus we consider a simpler problem & methodology:**
  - linear ion temperature gradient mode growth rates, electrostatic, low-beta, adiabatic electrons, no flows, $\eta_i = 10,\ L_n^{-1} = 2,\ L_T^{-1} = 20$
  - local equilibrium theory -- analytic, single surface only
  - ballooning/flux-tube, and assume Gaussian modes in analytics

Central question:

- ***How does one optimize the geometric properties of a surface along a field line for ITG modes?***

A proxy function for the growth rate is derived using analytic ITG theory

- **Ballooning/flux-tube limit, fluid limit $\omega/k_{||} >> v_{th,i}$, gyrokinetics theory (Romanelli 1989) yields ODE, cubic in eigenfrequency**

$$\hat{\omega}^3(1+\frac{b}{L_k^2}\hat{k}_\perp^2)\hat{\phi} - \hat{\omega}^2\frac{\sqrt{b}}{L_n}(1+2\frac{\rho L_n}{L_d^2}\hat{\omega}_d - W_K\frac{b}{L_k^2}\hat{k}_\perp^2)\hat{\phi}$$

$$+\hat{\omega}(-2W_K\frac{b}{L_d^2}\frac{\rho}{L_n}\hat{\omega}_d - \frac{1}{2}\frac{\rho^2}{L_{||}^2}\hat{k}_{||}^2)\hat{\phi} - W_K\frac{\sqrt{b}}{L_n}\frac{1}{2}\frac{\rho^2}{L_{||}^2}\hat{k}_{||}^2\hat{\phi} = 0$$

Geometric coefficients

- **Solve by averaging over eigenfunction,**

$$\langle f\rangle = \int_{\eta_i}^{\eta_f} d\eta \hat{\phi}^* f \hat{\phi} / \int_{\eta_i}^{\eta_f} d\eta |\hat{\phi}|^2,$$

$$\hat{\omega} = -\frac{\frac{\sqrt{b}}{L_n}(-1-2\frac{\rho L_n}{L_d^2}\langle\hat{\omega}_d\rangle + W_K\frac{b}{L_k^2}\langle\hat{k}_\perp^2\rangle)}{2(1+\frac{b}{L_k^2}\langle\hat{k}_\perp^2\rangle)} \pm \frac{\sqrt{\frac{\sqrt{b}}{L_n}(-1-2\frac{\rho L_n}{L_d^2}\langle\hat{\omega}_d\rangle + W_K\frac{b}{L_k^2}\langle\hat{k}_\perp^2\rangle)^2 + 4(1+\frac{b}{L_k^2}\langle\hat{k}_\perp^2\rangle)\cdot(2W_K\frac{b\rho}{L_d^2 L_n}\langle\hat{\omega}_d\rangle + \frac{1}{2}\frac{\rho^2}{L_{||}^2}\langle\hat{k}_{||}^2\rangle)}}{2(1+\frac{b}{L_k^2}\langle\hat{k}_\perp^2\rangle)}.$$

Only get $\gamma = \mathrm{Im}(\omega) > 0$ for $\langle\omega_d\rangle < 0$

Shaping controls the proxy target via the drift and FLR coefficients

- Result indicates squared growth rate scales like $\chi_{ITG}^2 = -\frac{\langle \hat{\omega}_d \rangle}{\langle \hat{k}_\perp^2 \rangle}$.

- **Drift coefficient**

$$\hat{\omega}_d = 2L_d^2 B_0 \frac{\kappa_n - \Lambda \kappa_g}{|\nabla \psi|}$$

- Normal curvature, geodesic curvature, torsion, and local shear

$$(\hat{\mathbf{b}} \cdot \nabla)\hat{\mathbf{b}} = \kappa_n \hat{\mathbf{n}} + \kappa_g \hat{\mathbf{b}} \times \hat{\mathbf{n}}$$
$$(\hat{\mathbf{b}} \cdot \nabla)\hat{\mathbf{n}} = -\kappa_n \hat{\mathbf{b}} + \tau_n \hat{\mathbf{b}} \times \hat{\mathbf{n}}$$
$$(\hat{\mathbf{b}} \cdot \nabla)\hat{\mathbf{b}} \times \hat{\mathbf{n}} = -\tau_n \hat{\mathbf{n}} - \kappa_g \hat{\mathbf{b}}$$
$$s = \hat{\mathbf{b}} \times \hat{\mathbf{n}} \cdot \nabla \times (\hat{\mathbf{b}} \times \hat{\mathbf{n}}).$$

- **FLR/polarization coefficient**

$$\hat{k}_\perp^2 = L_k^2 B_0^2 \frac{1 + \Lambda^2}{|\nabla \psi|^2}$$

- Parallel currents, P-S currents, local shear, and integrated local shear

$$\mu_0 \frac{\mathbf{J} \cdot \mathbf{B}}{B^2} = \sigma + p'\lambda$$
$$\mathbf{B} \cdot \nabla \lambda = 2\mu_0 \frac{|\nabla \psi|}{B} \kappa_g$$
$$s = \sigma + p'\lambda - 2\tau_n = \frac{g^{\psi\psi}}{B^2}\left(\frac{\iota'}{\sqrt{g}} + \mathbf{B} \cdot \nabla D\right)$$
$$\Lambda = \frac{\nabla S \cdot \nabla \psi}{B} = -\frac{g^{\psi\psi}}{B} \int_{\eta_k}^{\eta} d\eta \sqrt{g} \frac{B^2}{g^{\psi\psi}} s.$$

The instability scaling suggests three distinct shaping goals

Goals for shaping

1. Shift & maximize $\langle \frac{\kappa_n}{|\nabla\psi|} \rangle > 0$
2. Shift & maximize $\langle \frac{-\Lambda\kappa_g}{|\nabla\psi|} \rangle > 0$
3. Maximize $\langle \frac{\Lambda^2}{|\nabla\psi|^2} \rangle > 0$
   a. Minimize $|\nabla\psi|^2$

Physical meanings

Curvature drive

Geodesic curvature-torsion drive

Parallel/perpendicular coupling
Shear/FLR/polarization effects

- **Note that currents, global shear, and averaged torsion all related,**

$$\sigma = -\nu\hat{s} + 2\bar{\tau}_n \qquad \hat{s} = -B_0\rho^2\iota'/\iota \qquad \bar{\tau}_n = \langle B^2\tau_n/g^{\psi\psi}\rangle_{fs}/\langle B^2/g^{\psi\psi}\rangle_{fs}$$

- **Goal (2) implies rules for 2-D and 3-D (weak currents)**

$\kappa_g \cdot \int_{\eta_k}^{\eta} d\eta(\bar{\tau}_n - \tau_n) > 0$ for $\kappa_n < 0$ & $\hat{s} < 0$ — **2-D symmetry design rules**

$\kappa_g \cdot \int_{\eta_k}^{\eta} d\eta(\tau_n) < 0$ for $\kappa_n < 0$ — **3-D symmetry design rules**

Thus, relative phases of the curvatures and torsion are crucial.

Shaping mechanisms may be broadly categorized into a few general types

- **2-D: poloidal shaping (concavity & convexity control)**

  $$R = R_0 + \rho_0 \cos(\bar{\theta}) + \rho_1 \cos(M\bar{\theta}) + \cdots$$

- **3-D: three more fundamental mechanisms**
  - Axial translation

    $$R = R_0 + \rho_0 \cos(\bar{\theta}) + \rho_1 \cos(N\bar{\zeta}) + \cdots$$

  - Cross sectional rotation

    $$R = R_0 + \rho_0 \cos(\bar{\theta}) + \rho_1 \cos(M\bar{\theta} - N\bar{\zeta}) + \cdots$$

  - Cross sectional deformation (e.g. w/ rotation)

    $$R = R_0 + \rho_0 \cos(\bar{\theta}) + \rho_1 \rho_2 \cos(N_2\bar{\zeta}) \cos(M\bar{\theta} - N\bar{\zeta}) + \cdots$$

- **3-D shaping intimately tied to iota and (global) shear**
  - In 2-D, constraint is broken by currents

Note optimized stellarators usually show both rotation and deformation

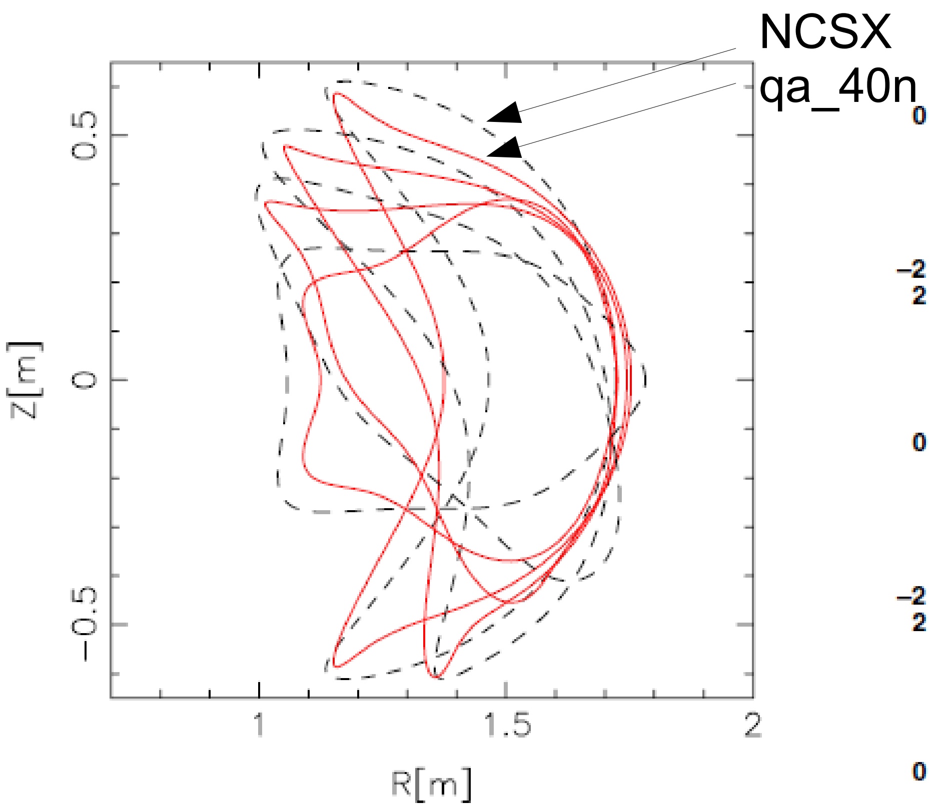

Mynick et. al., Physical Review Letters, 105 095004, 2010

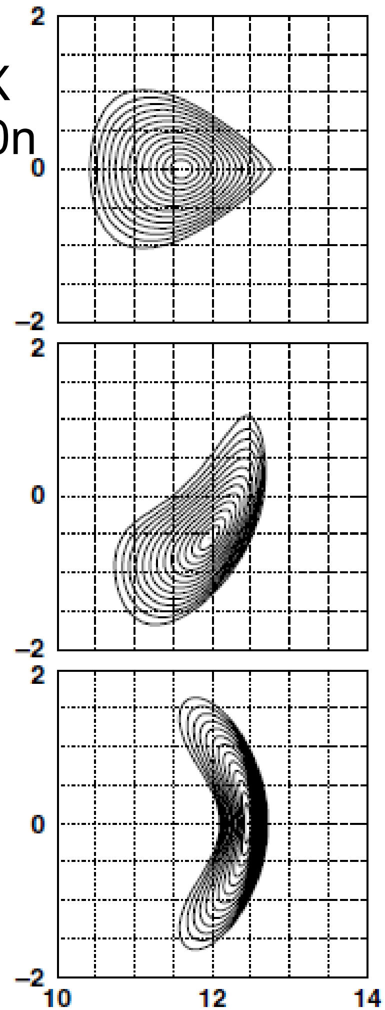

Subbotin et. al., Nuclear Fusion, 46 921, 2006

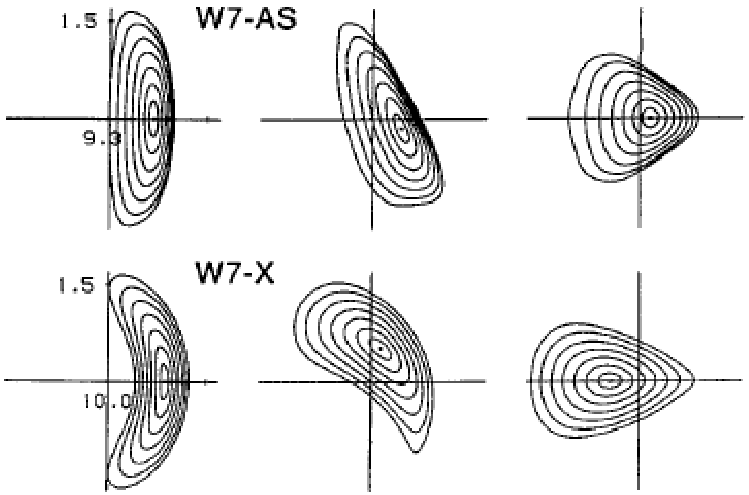

Grieger et. al., Phys. Fluids B, 4 2081, 1992

Curvature symmetries are controlled by edge positioning

Normal curvature | **Geodesic curvature** | **Normal torsion**

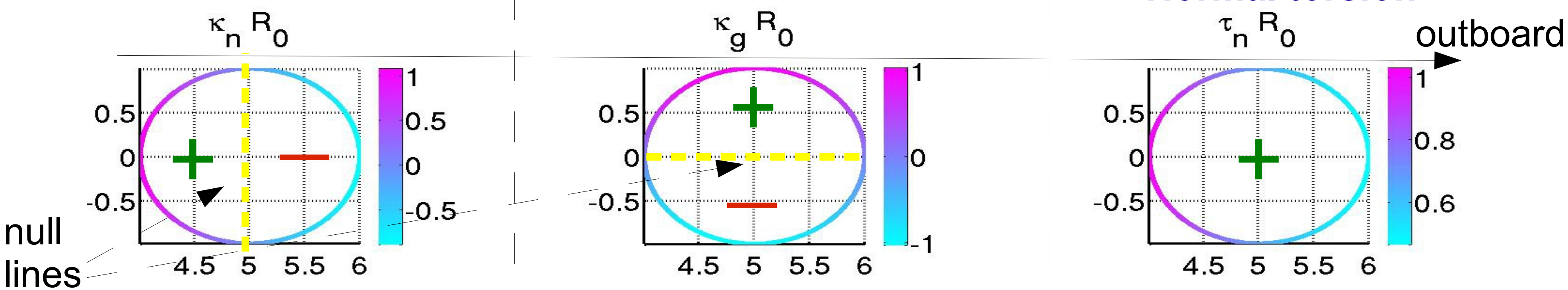

In 2-D, symmetry lines are typically left/right or up/down

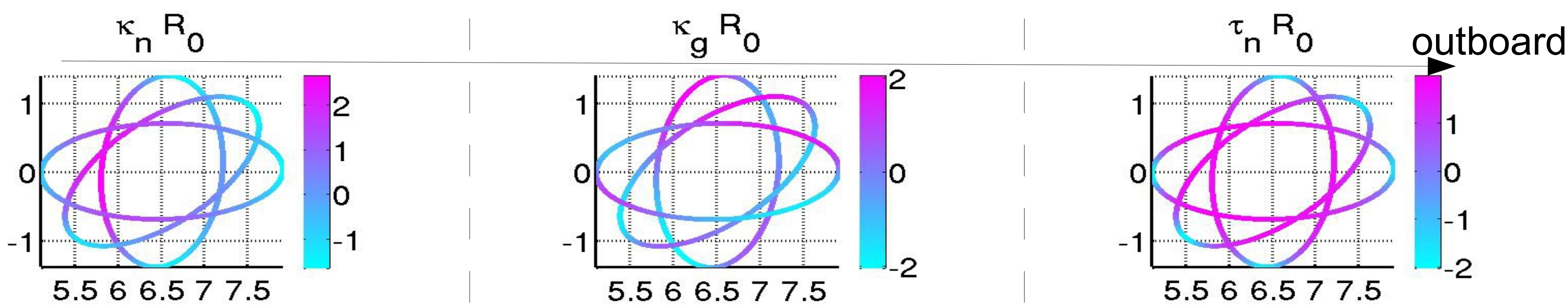

In 3-D, the symmetry lines follow corners/edges/cusps

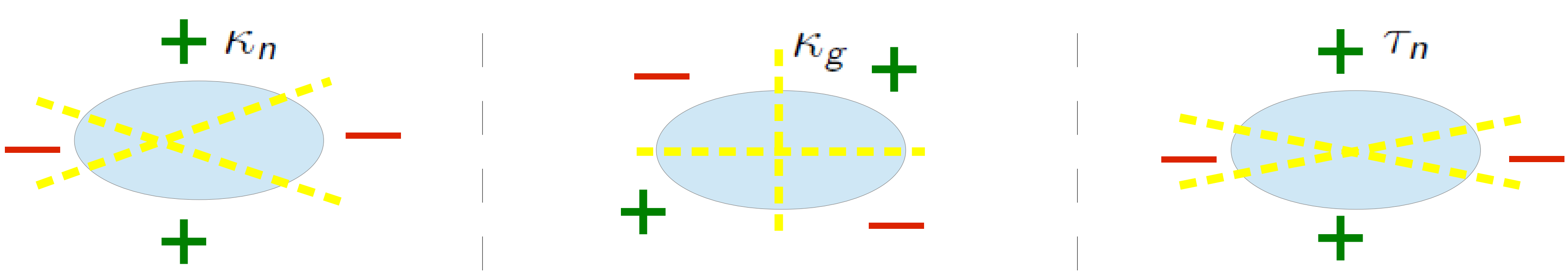

A framework for understanding is built up via selective example calculations

- **Analytic proxy results compared w/ numerical gyrokinetics GENE results using same equilibrium input**

- **Local equilibrium method checked against s-alpha model**

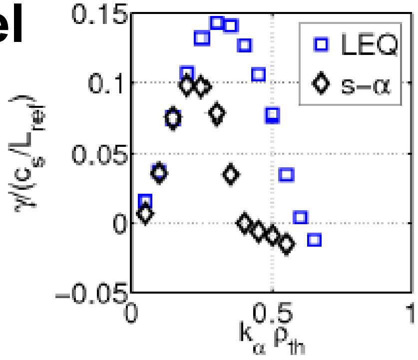

- **Simplifying assumptions for the rest of results:**
  - high gradients, $\eta_i = 10,\ L_n^{-1} = 2,\ L_T^{-1} = 20$
  - geometric angles are straight field line angles
  - limitation: manual parametrization of geometries

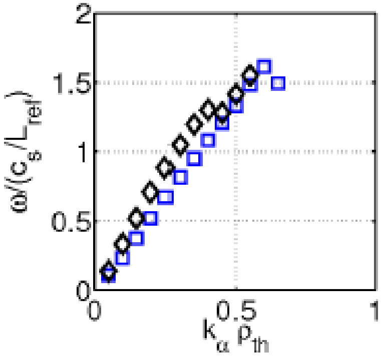

- **Focus on maximum linear growth rate -- scanning over ky-rho**

Concave inboard shaping yields both drift and FLR optimization

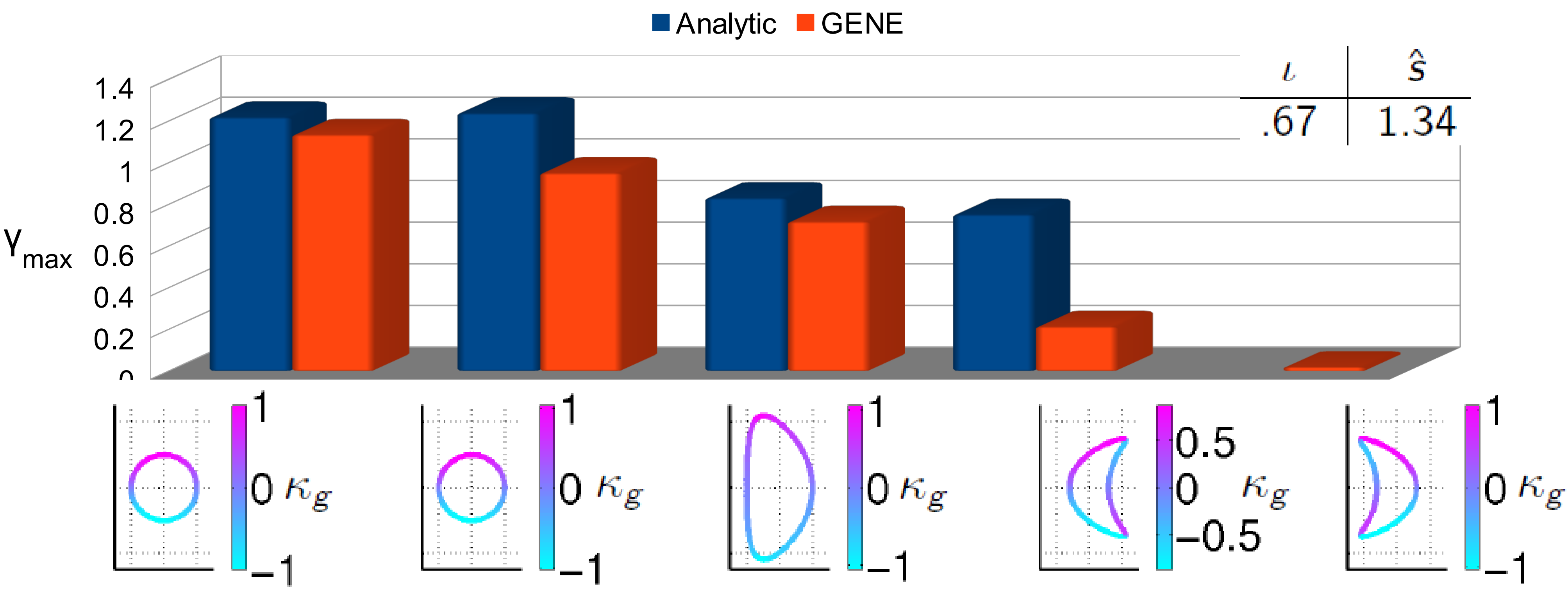

- **More averaged torsion & currents for cases 4,5 yield larger kperp^2**
- **Geodesic curvature phasing is optimal for case 5 vs. case 4**
- **Case 4 poor agreement – kinetic effects?**

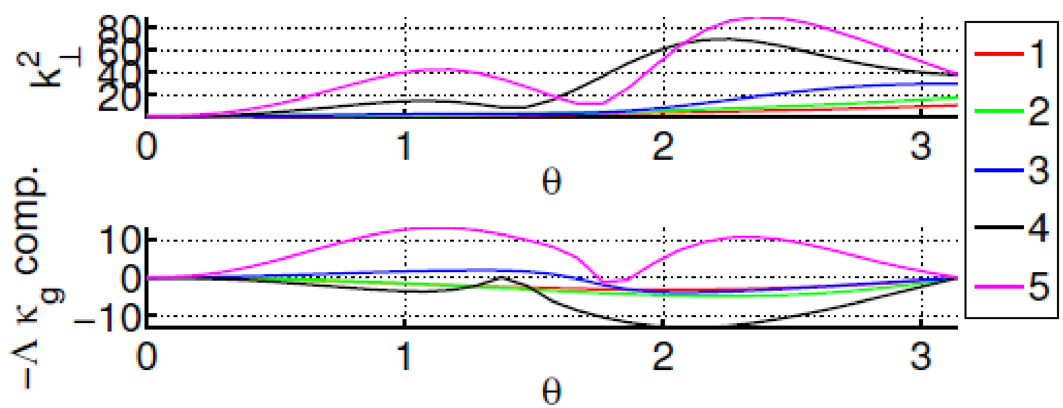

A few geometric quantities completely describe the surface

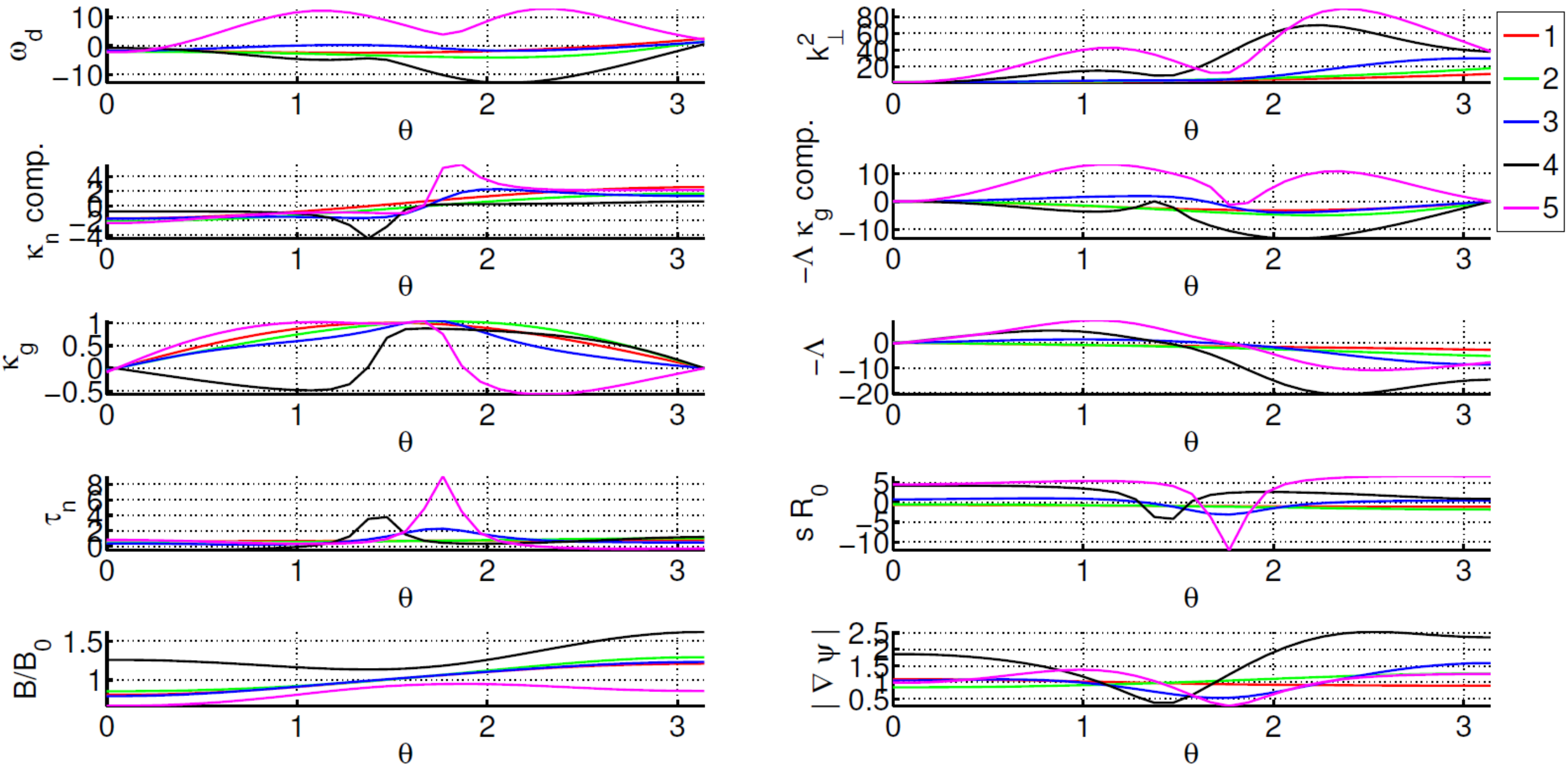

Can build intuition & completely analyze geometries with ~ 10 field line plots and handful of full surface plots.

Proxy result trends match GENE trends in stellarator geometry scans

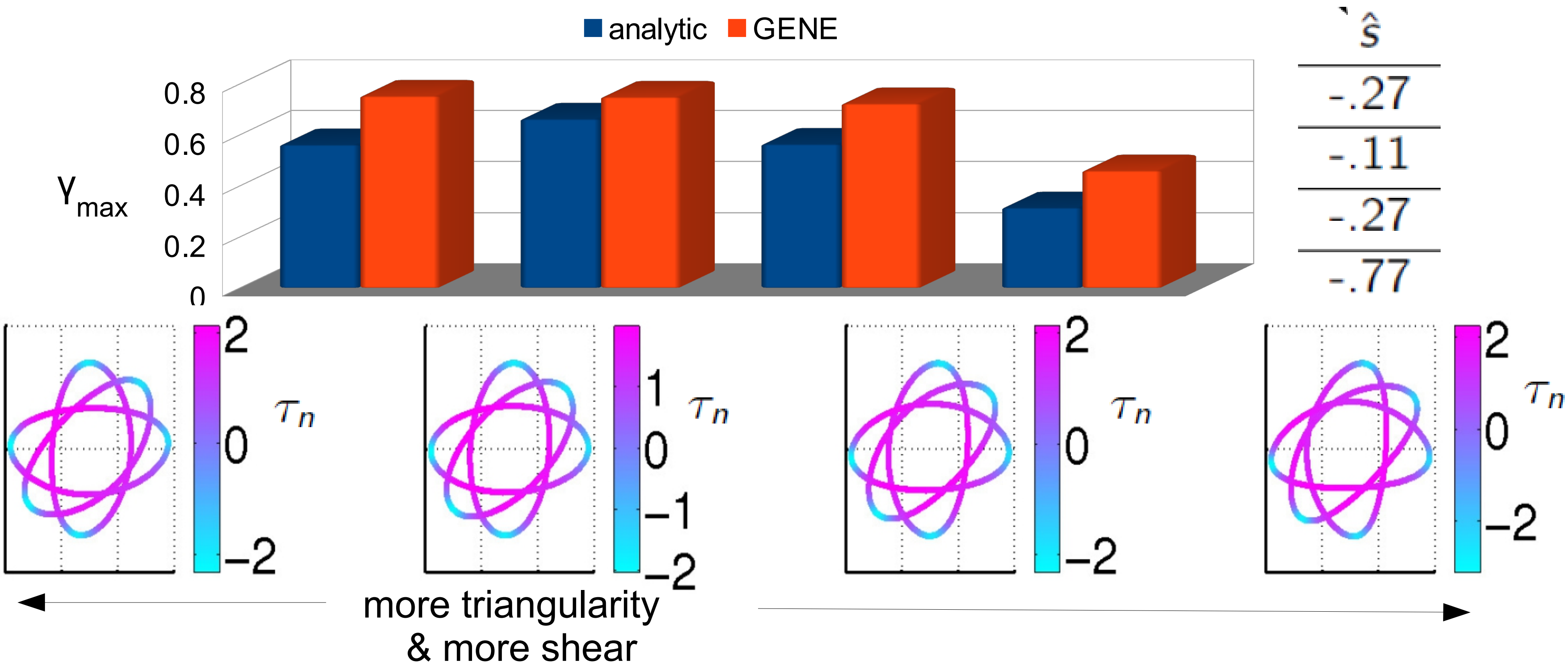

- **GENE results from domain extending 3 poloidal circuits (n_pol=3), proxy results with Gaussian full width of 3 poloidal circuits**
- **GENE shows only ~10% difference from n_pol=1 to 3**
- **Proxy misses trend on case 2 but geometries 1, 2, 3 all very similar**

GENE eigenfunctions clearly sit in w_d wells and k_perp^2 troughs

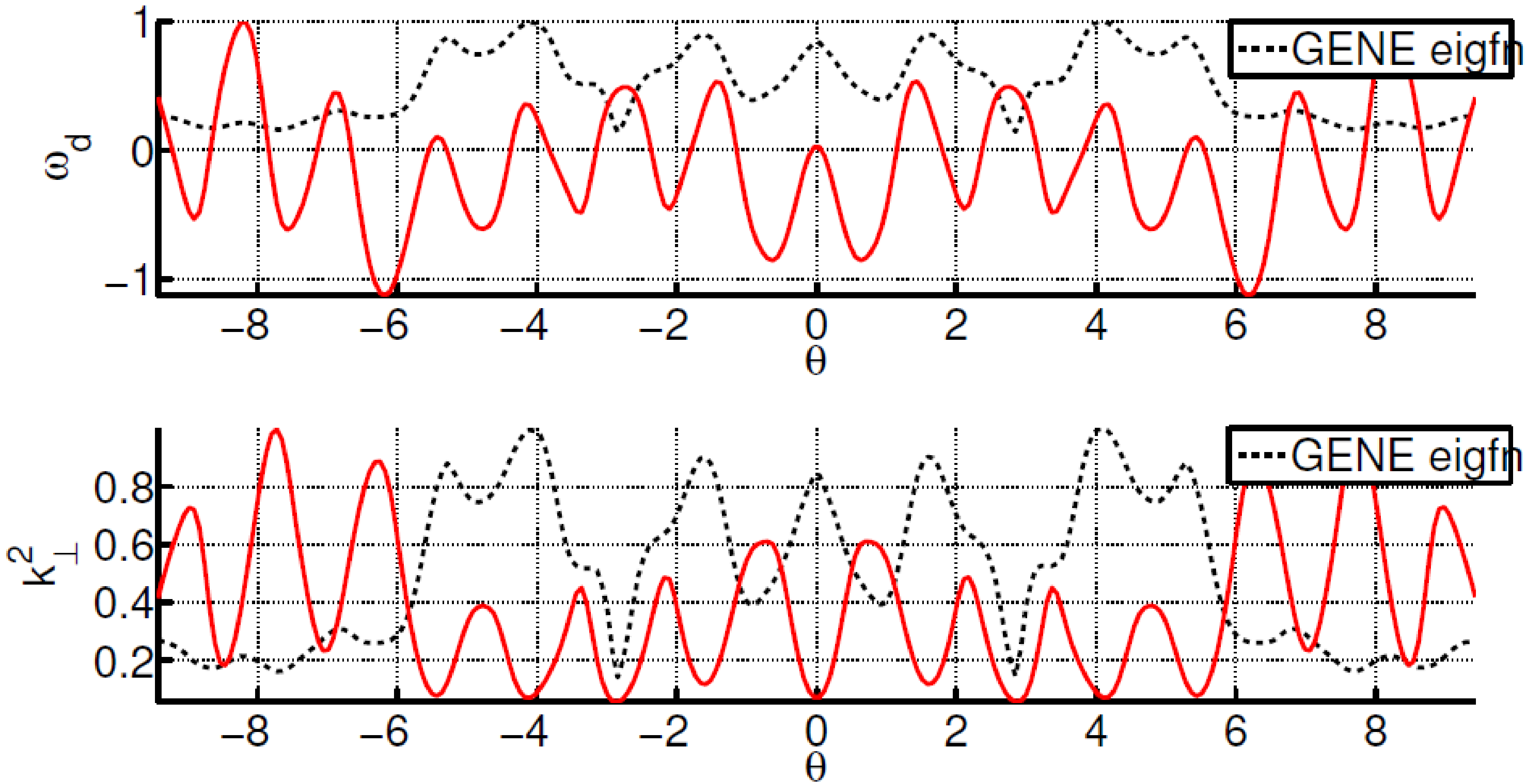

Extended GENE eigenfunction for case 2 (prev. slide), n_pol=3, against unitized values of w_d and k_perp^2

The analytic proxy growth rate can be sensitive to Gaussian mode width

Shear scan, circular tokamak -- shear destabilizes due to increase in curvature drive, spectra shrink to ky-rho =0

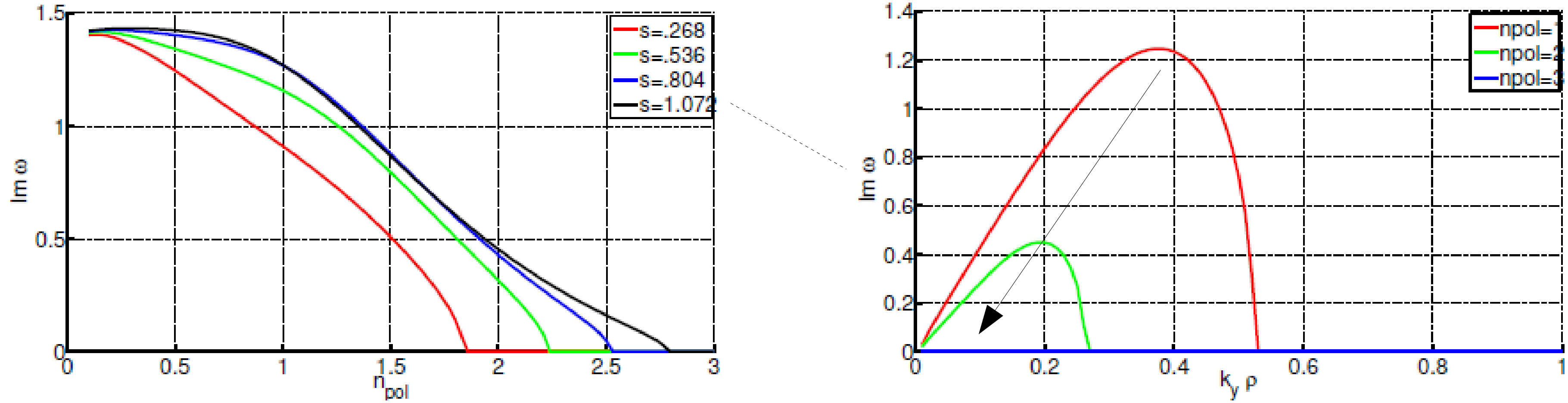

Elong. scan, N=10, m=1 stellarator -- shear stabilizes, gamma's converge due to spectral shift to smaller ky-rho & kperp^2 non-monotonic

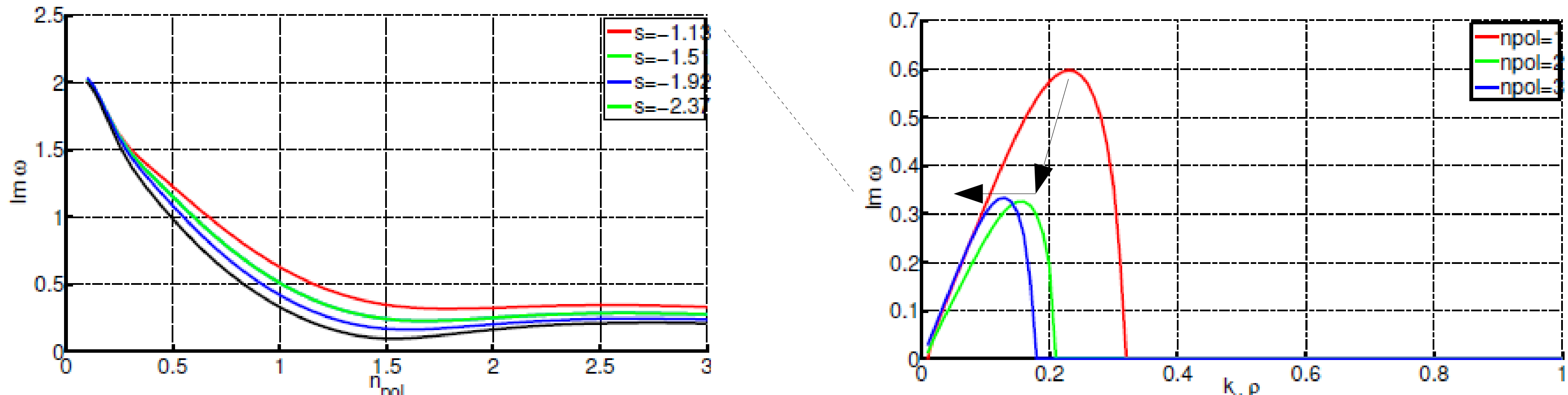

Deformation mechanism enables alteration of curvature symmetries

Deformation here causes the null lines to counter-rotate with respect to the surface

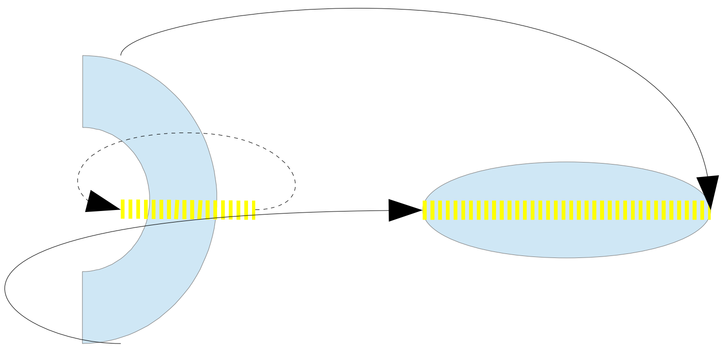

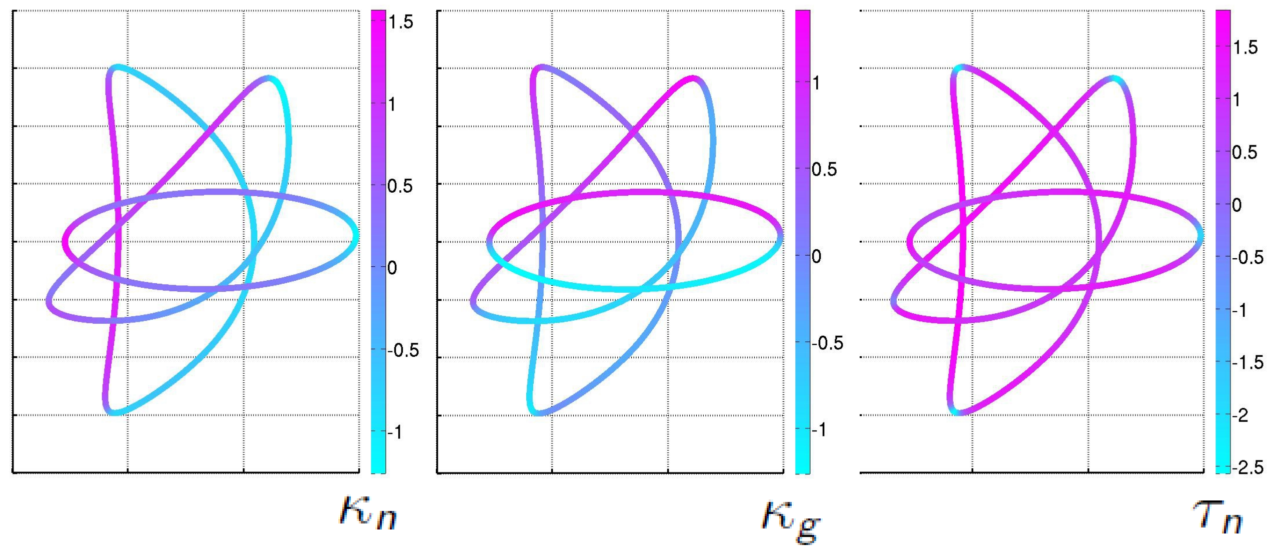

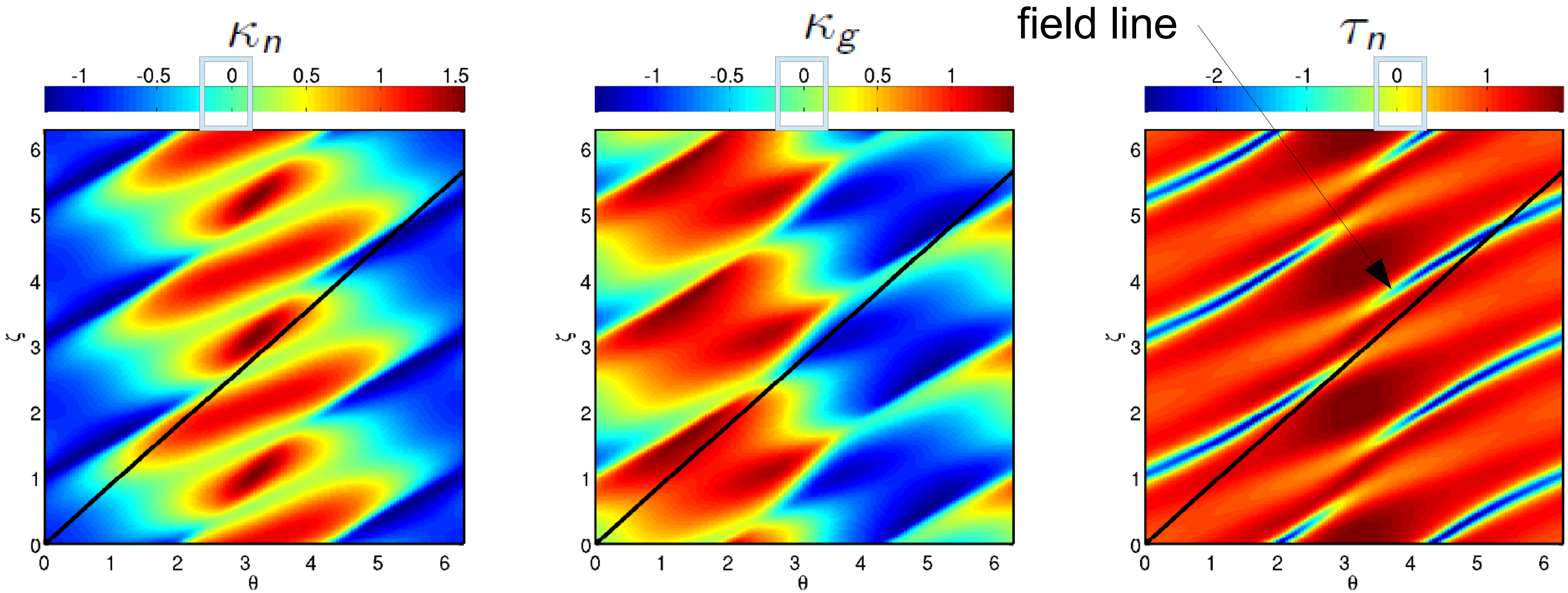

The helical curvature component is notably tuned out compared to a fixed M,N stellarator

Advanced shaping mechanisms necessitate numeric optimization

- **Local 3-D equilibrium theory developed for analytic parametrization of a single surface**
  - Good for simple shaping
  - Advanced shaping parametrizations cumbersome
- **Ex. (case from previous slide):**

$$R = R_0 + \rho_0 \cos(\theta)(1 + \rho_6 \cos(N_4\zeta)^2) + \rho_2 \cos(\theta - N\zeta)$$
$$+ \rho_3 \cos(2\theta - N_2\zeta - \pi/2) \sin(N/2\zeta) + \rho_5 \cos(M\theta - N_3\zeta) \sin(N/2\zeta)^2$$
$$+ \delta \cos(N\zeta)$$

$R_0 = 6.5, \rho_0 = 1.05, \rho_6 = -0.2, N_4 = .5N, \rho_2 = 0.4\rho_0, N = 3, \rho_3 = 0.5\rho_2, N_2 = 1.5N, \rho_5 = -0.2\rho_3, N_3 = 2N, \delta = 0.2\rho.$

- **Harmonics:** 1 pure poloidal, deformational, rotational, and translational, and 2 simultaneous rotational + deformational

Deformation shaping improves on M=1 shape at the outboard 'shoulder'

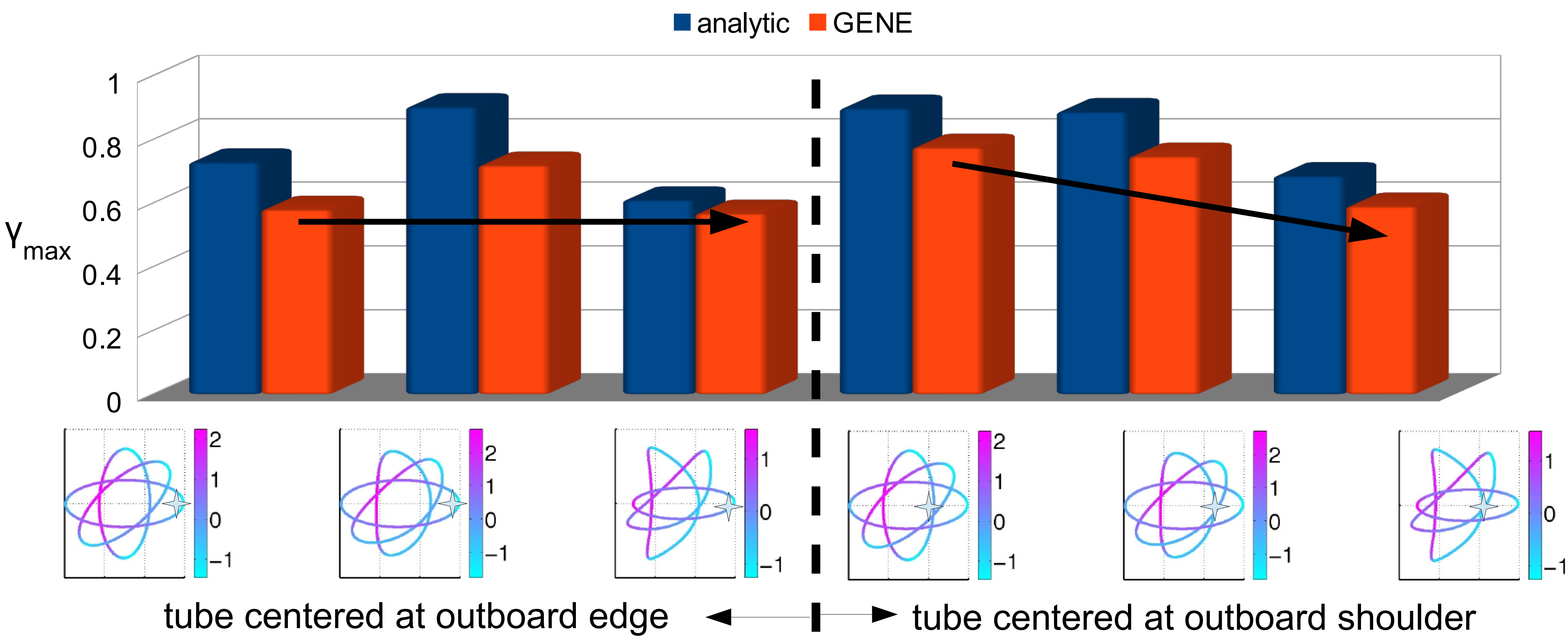

Keeping the torsion single-signed longer allows larger integrated shear: more stability.

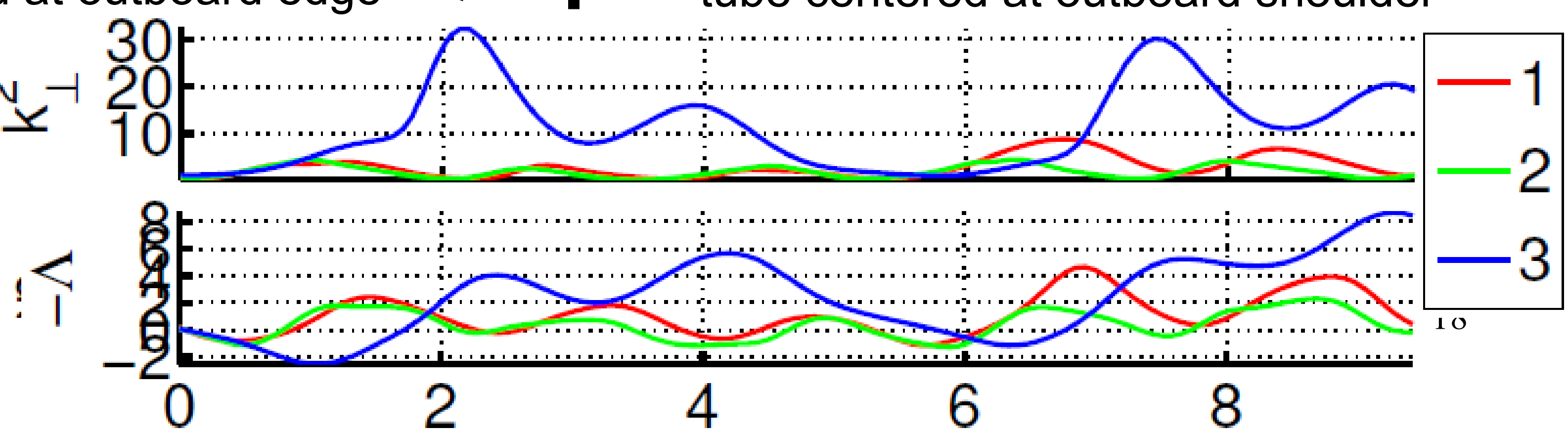

Kinetic effects appear mostly unimportant in these parameter regimes

- **Analytic model tracks trends despite lacking resonant kinetic contributions**
  - Possible explanations:
    - Not in the right parameter regime -- only important near threshold?
    - Modes too extended -- i.e. need smaller $\lambda_{||}$?
      - Investigation with numerical experiments:

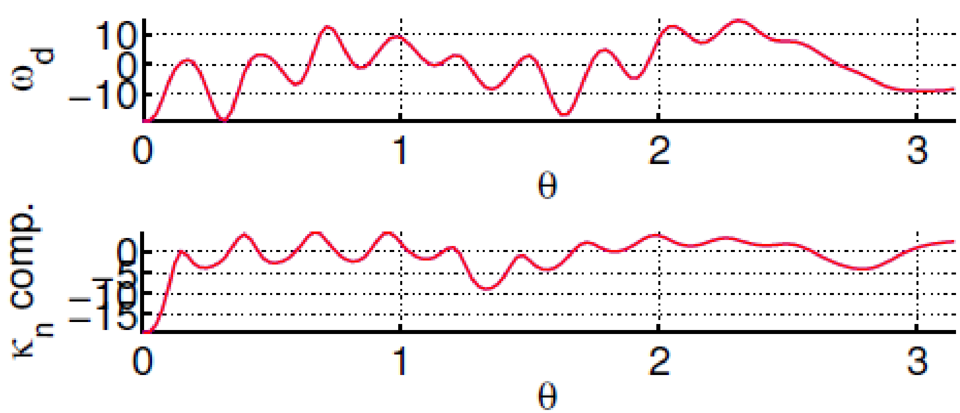

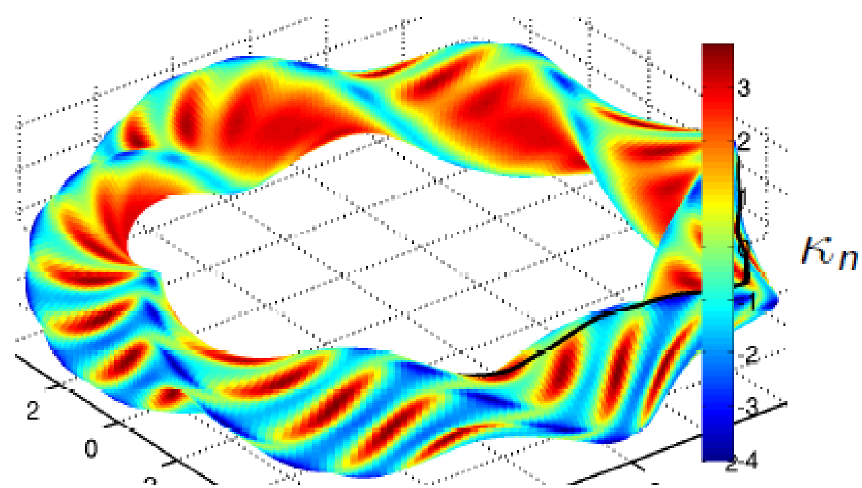

Even with connection length approx. 10x shorter than tokamak, proxy still accurately tracks GENE trends

Conclusions

i. Fluid-based targets have been investigated

- Scale generally with curvature and FLR terms

ii. Framework for geometric understanding shown

- Symmetry patterns dictated by edge locations in 3-D
  - May be fundamentally altered & tailored via shaping

iii. Analytic model predicts GENE trends

- Mode width important in proxy, less so in GENE

iv. Results suggest continuum of shaping effects

- Geodesic curvature-torsion optimization shows promise

v. Results translate directly to STELLOPT proxy & output analysis

Future work

Shortest term

- Write up results for paper & do prelim
- Translate proxy for current STELLOPT implementation (Mynick et. al.)
- Support & collaborate in HSX optimization inquiries

Medium term

- More analytic focus – helps untangle large parameter space
  - Analytic proxies for TEM type modes & kinetic effects
  - Better estimates of mode lengths
  - Better understanding of global behavior (one tube vs. another)

Longer term

- Nonlinear optimization targets -- existence, implications, etc.
  - Can the nonlinear physics be optimized?